A Non-Pilot Aided Iterative Carrier Frequency Offset Estimator Using Optimal Filtering for an Interleaved OFDMA Uplink System

Hector Poveda, Guillaume Ferré, Eric Grivel

Wireless Pers Commun
DOI 10.1007/s11277-011-0480-7

A Non-Pilot Aided Iterative Carrier Frequency Offset Estimator Using Optimal Filtering for an Interleaved OFDMA Uplink System

Héctor Poveda · Guillaume Ferré · Eric Grivel

Abstract In an uplink transmission of a coded orthogonal frequency division multiple access (C-OFDMA) system, channel estimation, time and frequency synchronization has to be addressed. For this purpose a control data, i.e. a known training sequence called "preamble" and pilot sub-carriers are used. As an alternative to the classic scheme and in order to maximize the data rate, we propose a non-pilot aided estimator based on an iterative architecture that does not require pilot sub-carriers. Our approach combines 1/ the so-called minimum mean square error successive detector to estimate the signal sent by each user 2/ a recursive method estimating the CFOs. Various algorithms such as the extended Kalman filter, the sigma-point Kalman filters and the extended H_∞ filter are tested and their performances are compared in terms of convergence speed and estimation accuracy. When considering an interleaved OFDMA uplink system over a Rayleigh fading channel, simulation results clearly show the efficiency of the proposed algorithm in terms of CFO estimation and bit error rate performances.

Keywords OFDMA · Extended Kalman filter · Sigma-point Kalman filter · Extended H_∞ filter · Carrier frequency offset

1 Introduction

Multiuser orthogonal frequency division multiplexing (OFDM) system, also known as orthogonal frequency division multiple access (OFDMA), is used in many new

H. Poveda (✉) · G. Ferré · E. Grivel
Equipe Signal et Image, IPB-ENSEIRB-MATMECA, UMR CNRS 5218 IMS,
Université Bordeaux 1, 351 cours de la libération, 33405 Talence Cedex, France
e-mail: hector.poveda@ims-bordeaux.fr

G. Ferré
e-mail: guillaume.ferre@ims-bordeaux.fr

E. Grivel
e-mail: eric.grivel@ims-bordeaux.fr

Published online: 20 December 2011

communication standards, such as WiMAX (802.16x) [1] and 3GPP long-term evolution (LTE) for the downlink [2]. Unlike the conventional OFDM case where all sub-carriers are assigned to a single user, each sub-carrier is exclusively assigned to a particular user in an OFDMA network. The communication link between each user and the base station is modeled by a time-varying channel, whose response differs from one user to another. For simultaneous transmissions, OFDMA allocation algorithms [3] aim at exploiting this spectral diversity to allocate to the different users the communication resources, such as power, constellation size and necessary bandwidth to maximize the link efficiency. However, like OFDM, OFDMA is sensitive to:

– timing errors between the incoming signal and the base station (BS) references used for reception and demodulation in the uplink case: they lead to inter-block interferences (IBI) and can be avoided by using a sufficiently long cyclic prefix between two adjacent OFDMA bursts. However, to maintain acceptable data throughput, the cyclic-prefix length must be chosen just greater than the length of the channel impulse response (CIR).
– carrier frequency offsets (CFOs): without CFO estimations and compensations, orthogonality between sub-carriers is no longer satisfied; this results in inter-channel interferences (ICI) as well as multiple access interferences (MAI).

The above problems have to be solved during an OFDMA transmission. Timing synchronization, CFO estimation, MAI correction and channel estimation are performed using a known training sequence called "preamble" composed of a few OFDMA symbols at the beginning of the OFDMA frame. Then, pilot sub-carriers are inserted in the frame to make the coherent detection robust against variations of CFOs over the frame. See Fig. 1.

The CFO estimation problem for OFDMA uplink transmissions using the preamble has been recently addressed in several papers. In [3], Morelli et al. illustrate various schemes for CFO estimation among different sub-carrier allocation strategies. In [4], the CFO estimation is obtained by comparing the phases of two identical received OFDMA symbols. In [5], Zhao et al. use an extended Kalman filter (EKF) to estimate the CFO. However, channels are assumed to be preliminarily estimated and this assumption is not necessarily satisfied in real cases. Indeed, during the uplink synchronization stage, the channel state information (CSI) is not available, and hence has to be estimated either jointly with the CFO or after CFO compensation.

In order to correct the MAI, the CFO has to be compensated. In the so-called "direct method", the CFOs are compensated by multiplying the complex envelope of the signal before the fast Fourier transform (FFT) step at the receiver. However, there is a performance

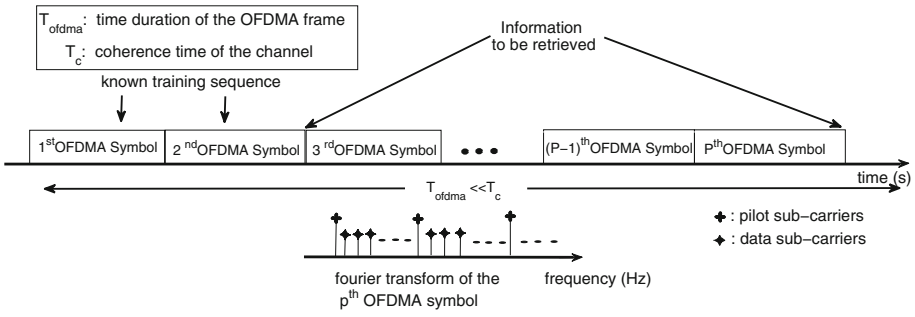

Fig. 1 Example of an OFDMA frame composed of P OFDMA symbols with a preamble composed of two OFDMA symbols and a determined number of pilot sub-carriers

degradation because the CFO compensation of the desired user may increase the CFOs of the other users. As an alternative, new correction methods have been proposed. More particularly, in [6] the CFO compensation is implemented by mitigating the effects of the major lobes and the side lobes of the frequency response of the signals received from each user. The CFO estimation can be obtained calculating the phase shifts of two identical received OFDMA symbols in the time domain. In [7], CFO compensation is based on a circular convolution after the FFT step. The authors suggest using the method presented in [8] to estimate the CFOs. However, both methods only work for subband carrier allocation strategy (CAS). Consequently, in [9], the authors extend the concept proposed in [7] to a system with interleaved or generalized CAS. In that case, the CFOs are corrected via a circular convolution after the FFT step, but an interference-cancellation step is required. The authors suggest again to use the method presented in [8] to estimate the CFOs. In [10], the authors carry out the CFO correction through a linear detection and the CFO estimation is performed by using a high-resolution subspace method. In [11], Hou et al. propose a minimum mean square error successive detector (MMSE-SD) to suppress the MAI, but the CFO is assumed to be known.

In the above approaches channel estimation is not included. The joint CFO/ channel estimation has been also investigated. In [12] and [13], Pun et al. study how to obtain the joint maximum likelihood estimations of the channels and the CFOs of multiple users. Thus in [12], a conventional expectation-maximization (EM) is first proposed: during the E-step the received signals transmitted by each user, namely the "complete data", are estimated. During the M-step, all the CFOs and the channels are jointly estimated by using these complete data. To simplify the optimization issue, the value of the channel is replaced by its expression depending on the CFO in the criterion to be minimized. Therefore, only the CFO of each user has to be estimated. Even if the criterion is explicitly given, the authors do not mention the estimation method used. For instance, exhaustive grid search could be considered as suggested by the same authors in [13]. To reduce the computational cost, the authors in [12] suggest using the space alternating generalized expectation-maximization (SAGE). In that case, instead of simultaneously estimating every-user parameters, one iteration of the EM algorithm is dedicated to one user. Instead of addressing a multi-dimensional optimization issue, the authors in [13] use the so-called alternating projection estimator. This method consists in iteratively estimating the CFO of one user, by means of an exhaustive grid search over the possible range of the CFO value, and by setting the other CFOs to their last updated values. In [14], Xiaoyu et al. propose two iterative estimation approaches using the SAGE method. Nevertheless, the EM-based algorithms do not necessarily converge to the global extremum. An initialization step is therefore required. Another drawback of the above methods is the high computational cost due to the iterative estimation and the exhaustive grid search. To obtain a maximum data rate, alternative estimation approaches using the preamble and pilot sub-carriers have been proposed. In [15], the authors propose a subspace based blind CFO estimation algorithm. It consists of a high-resolution signal-processing technique to estimate the CFO without pilot sub-carriers. Nevertheless, more sub-channels than users are required. For certain values of CFOs, a grid search approach leads to a sub-optimal estimation. In [16], a blind method to estimate CFOs based on a linear precoder is proposed. Using two OFDMA symbols, the idea is to establish a time correlation using a precoder which gives a second-order moment based blind CFO estimation for each user.

In the above approaches, the OFDMA frame duration is usually higher than the coherence time (T_c) of the channel. In this case, the CSIs need to be updated by using pilot sub-carriers. In this paper, we suggest using a shorter OFDMA frame so that the CSIs do not change. The sub-carriers are no longer necessary to update the CSIs and can be removed. The data rate is hence increased, but the CFO may vary from one symbol to another. Then, we propose

a non-aided iterative receiver that combines an MMSE-SD with a CFO estimator based on optimal filtering. It should be noted that the preamble is kept (in order) to perform the timing synchronization, to estimate the CSI for the whole frame and to provide an initial estimation of the CFO.

To compare estimation performances, four CFO estimation methods dedicated to non-linear estimation are studied: on the one hand, we analyze the relevance of local estimation methods such as the extended Kalman filter (EKF) and the extended H_∞ filter [17], which are based on a first-order linearization of the state-space representation of the system around the last available state estimation. On the other hand, we investigate estimation methods such as the sigma-point Kalman filters [18] including the unscented Kalman filter (UKF) and the central difference Kalman filter (CDKF).

The paper is organized as follows. The OFDMA system and the signal models are presented in Sect. 2. Section 3 shows how estimates of the synchronization parameters can be exploited to restore orthogonality among the received user signals. In Sect. 4, the computational complexity of the proposed algorithm is addressed. In Sect. 5, various simulations have been performed. Firstly, the channel is assumed to be exactly known. The results obtained confirm the efficiency of our approach. Then, the influence of the channel estimation error on the CFO estimator is studied. In Sect. 6, conclusions are drawn and perspectives are given. Appendix A highlights the differences between Kalman filtering and H_∞ filter, whereas Appendix B provides details about SPKF.

In the following, $(.)^H$, $(.)^T$ and $(.)^*$ denote the hermitian, transposition and conjugate operations respectively. In addition $Re(.)$ denotes the real part of $(.)$, diag$(.)$ is a square zero matrix, the main diagonal of which is $(.)$ and $\mathbf{I}_q$ is the identity matrix of size q.

2 System Description

Let us consider an OFDMA network consisting of a single BS and U simultaneously independent users. See Fig. 2. The available bandwidth B is divided among N sub-bandwidth, and we assume its fair distribution between each user, namely $B_u = B/U$.

The signal received by the BS is a superposition of the contributions from the U active users. In the following, let $\mathbf{S}_u$ be the OFDMA symbol emitted by the uth user with $u \in \{1, \ldots, U\}$:

$$\mathbf{S}_u = [S_u(0), S_u(1), \ldots, S_u(N-1)]^T \tag{1}$$

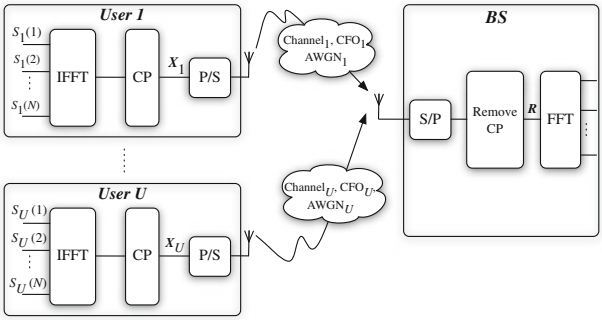

Fig. 2 OFDMA system model

According to the frequency allocation of each user [3], $S_u(k)$ is non-zero if the kth carrier is allocated to the uth terminal mobile, for $k \in \{0, \ldots, N-1\}$. Then, let us introduce the column vector $\mathbf{S}$ that contains the information symbols to be transmitted along the N sub-carriers:

$$\mathbf{S} = \mathbf{S}_1 + \mathbf{S}_2 + \cdots + \mathbf{S}_U \tag{2}$$

The corresponding transmitted signal from the uth user is given by:

$$X_u(n) = \frac{1}{\sqrt{N}} \sum_{k=0}^{N-1} S_u(k) e^{j2\pi nk/N} \tag{3}$$

where $-N_g \leq n \leq N-1$ and $N_g < N$ is the length of the cyclic prefix (CP). Moreover, let us assume that the channel impulse response of the uth user at time n is $\mathbf{h}_u = [h_u(0), h_u(1), \ldots, h_u(L_u - 1)]^T$ where L_u is the length of the maximum channel delay spread and $N_g \geq \underset{u}{max}(L_u)$ so that the cyclic prefix discards the IBI. We suppose a multipath Rayleigh quasi-static frequency selective channel. Hence, $\mathbf{h}_u$ does not vary during an OFDMA frame.

The U incoming waveforms are naturally combined by the receiver antenna. The resulting received signal at time n can hence be expressed as follows:

$$R(n) = \sum_{u=1}^{U} R_u(n) + B(n) \tag{4}$$

where $B(n)$ is a complex white Gaussian noise with zero mean and variance σ_b^2 while $R_u(n)$ is the signal received from the uth user. At the receiver, due to the propagation conditions, time offset and CFO are induced in the baseband signal. As presented by Morelli in [3], the received signal after the cyclic prefix removal can be written as follows:

$$R_u(n) = \frac{1}{\sqrt{N}} \sum_{k=0}^{N-1} S_u(k) H_u(k) e^{j2\pi n(k+\epsilon_u)/N} \tag{5}$$

where $H_u(k) = \sum_{l=0}^{L_u-1} h_u(l) e^{-j2\pi(lk+\tau_u k+\tau_u\epsilon_u)/N}$ is the channel frequency response associated to the kth sub-carrier of the uth user and with ϵ_u and τ_u the normalized CFO to the sub-carrier spacing and the timing error related to the uth user, respectively.

To restore orthogonality among each user sub-carrier, the synchronization error vector ϵ must be estimated to compensate the CFOs.

$$\epsilon = [\epsilon_1, \epsilon_2, \ldots, \epsilon_U] \tag{6}$$

By choosing an appropriate cyclic prefix length, namely $N_g = \max_u \{\tau_u + L_u\}$, the effects of the uplink timing errors are counteracted, i.e they are incorporated as a part of their channel responses. [1] Thus, the received signal contains no IBI and (4) can be rewritten as:

$$R(n) = \sum_{u=1}^{U} e^{j2\pi n\epsilon_u/N} A_u(n) + B(n) \tag{7}$$

[1] τ_u and L_u are supposed to be known. The signal is assumed to be synchronized in time.

where $A_u(n)$ corresponds to the nth sample of the OFDMA symbol only affected by the propagation channel and which can be expressed as:

$$A_u(n) = \frac{1}{\sqrt{N}} \sum_{k=0}^{N-1} S_u(k) H_u(k) e^{j2\pi nk/N} \tag{8}$$

By using (4), each received OFDMA symbol can be rewritten in a matrix form as follows:

$$\mathbf{R} = [R(0), R(1), \ldots, R(N-1)]^T = \mathbf{GS} + \mathbf{B} \tag{9}$$

where $\mathbf{B} = [B(0), B(1), \ldots, B(N-1)]^T$ is a column vector that contains N consecutive samples of the additive noise. In addition, the $N \times N$ transmission matrix $\mathbf{G}$ is defined by:

$$\mathbf{G} = \sum_{u=1}^{U} \mathbf{E}_u \mathbf{H}_u \mathbf{Q}_u \tag{10}$$

where:

$$\mathbf{E}_u = \text{diag}\left[1, e^{j2\pi\epsilon_u/N}, \ldots, e^{j2\pi(N-1)\epsilon_u/N}\right] \tag{11}$$

$\mathbf{Q}_u$ is a diagonal matrix where the kth coefficient of the main diagonal is given by:

$$\mathbf{Q}_u(k,k) = \begin{cases} 1 & \text{if } S_u(k) \neq 0 \\ 0 & \text{elsewhere} \end{cases} \tag{12}$$

and

$$\mathbf{H}_u = \begin{bmatrix} H_u(0) & H_u(1) & \ldots & H_u(N-1) \\ H_u(0) & H_u(1)e^{\frac{j2\pi}{N}} & \ldots & H_u(N-1)e^{\frac{j2\pi(N-1)}{N}} \\ \ldots & \ldots & \ldots\ldots & \\ H_u(0) & H_u(1)e^{\frac{j2\pi(N-1)}{N}} & \ldots & H_u(N-1)e^{\frac{j2\pi(N-1)^2}{N}} \end{bmatrix} \tag{13}$$

Due to the CFO, the received OFDMA symbol column vector $\mathbf{R}$ includes interferences both from the user itself and from all the other users.

In the next section, we analyze the way to estimate the CFO and to correct the MAI in order to obtain the decoded signals of each user.

3 Frequency Offset Estimation and User Detection

In uplink OFDMA systems after performing the CFO/channel estimation using the preamble, receiver performances could be affected by the MAI caused by the CFO variations over all the OFDMA frame. In this section, a method is proposed to mitigate this impact.

The idea is to correct the MAI and to estimate the signals sent from all users in the system using the MMSE-SD. These estimated signals called the "MMSE-SD preambles" play the role of the pilot sub-carriers and are used to estimate the CFOs using the optimal filtering. [2] See Fig. 3.

It should be noted that the preamble is kept to perform the timing synchronization, to estimate the CSI for the whole frame and to provide an initial estimation to the CFO. See Fig. 4.

[2] It should be noted that a preliminary study was presented in [19].

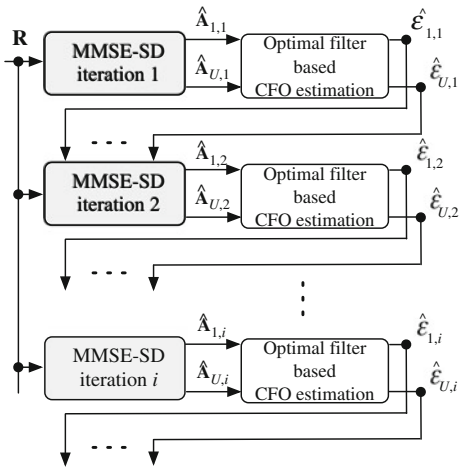

Fig. 3 Proposed OFDMA receiver architecture using optimal filter estimator

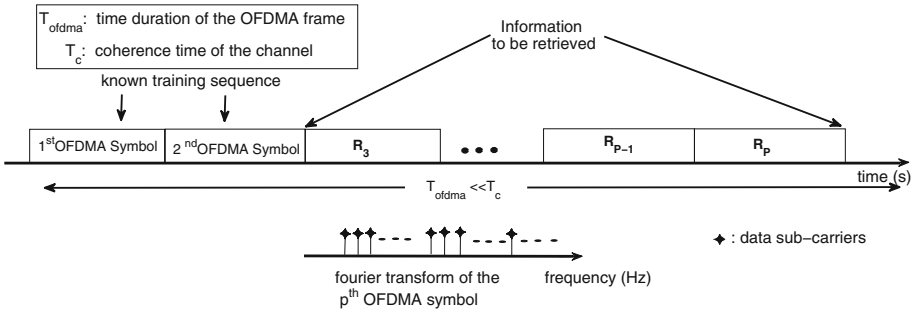

Fig. 4 OFDMA frame composed of P OFDMA symbols with a preamble composed of two OFDMA symbols and no pilot sub-carriers

3.1 MAI Suppression MMSE Successive Detection

According to [11], the MMSE-SD is robust against near-far effect, produced by the strong MAI. These phenomena are induced by the difference that may exist between two users in terms of the propagation loss. Instead of a joint multiuser decoding, we propose to combine a MMSE pre-detection scheme with an ordered successive detection. The detection of transmitted interleaved OFDMA signal components operates in two major steps:

– interference cancelling (IC): during this step, the previous "detected" OFDMA signal components are subtracted out of the received signal. Indeed, let $\hat{\mathbf{S}}_{\tilde{u},i}$ be the estimation of the signal sent by the $\tilde{u}$th user at the ith iteration of the MMSE-SD, where $1 \leq i \leq I_{max}$ and I_{max} denotes the maximum iteration number. The user's decoding order is denoted as $\tilde{u}$ where $\tilde{u} \in \{1, \ldots, U\}$; when $\tilde{u} = 1$, it is associated with the maximum signal to interference-plus-noise ratio [3] (SINR) among the users whereas $\tilde{u} = U$ represents the user with the lowest SINR. In addition the so-called $(\tilde{u}+1)$th order MMSE-SD residual at the ith iteration $\mathbf{Y}_{\tilde{u}+1,i} \forall \tilde{u} \neq 1$ is the difference between the received signal $\mathbf{R}$ and the components transmitted by the detected users (namely those corresponding to the $\tilde{u}$ highest SINRs) and $\mathbf{Y}_{1,i} = \mathbf{R} \forall i$. See Fig. 5.

[3] The BS calculates the SINRs, then the signal is decoded in an ordered way [11].

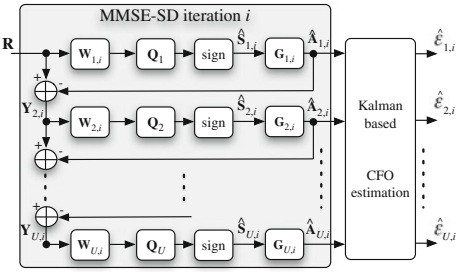

Fig. 5 Iterative MMSE-SD using Kalman filter estimator and MAI suppression for BPSK modulation

The IC steps can be summarized as follows:

$$\mathbf{Y}_{\tilde{u}+1,i} = \mathbf{Y}_{\tilde{u},i} - \hat{\mathbf{G}}_{\tilde{u},i}\hat{\mathbf{S}}_{\tilde{u},i} \tag{14}$$

$$= \mathbf{R} - \sum_{l=1}^{\tilde{u}} \hat{\mathbf{G}}_{l,i}\hat{\mathbf{S}}_{l,i} \tag{15}$$

$$\text{with } \hat{\mathbf{G}}_{\tilde{u},i} = \begin{cases} \sum_{\tilde{u}=1}^{U} \hat{\mathbf{E}}_{\tilde{u},i}\mathbf{H}_{\tilde{u}}\mathbf{Q}_{\tilde{u}} & \text{if } \tilde{u} = 1 \\ \hat{\mathbf{G}}_{\tilde{u}-1,i}\left(\mathbf{I}_N - \mathbf{Q}_{\tilde{u}-1}\right) & \text{if } 2 \le \tilde{u} \le U \end{cases} \tag{16}$$

where $\hat{\mathbf{E}}_{\tilde{u},i} = \text{diag}\left[1, e^{j2\pi\hat{\epsilon}_{\tilde{u},i-1}/N}, \ldots, e^{j2\pi(N-1)\hat{\epsilon}_{\tilde{u},i-1}/N}\right]$ and $\hat{\epsilon}_{\tilde{u},i}$ is the estimation of the CFO associated with the $\tilde{u}$th user at the ith iteration. [4] A new iteration begins when all the users have been processed and when the estimation $\hat{\epsilon}_{\tilde{u},i}$, using the recursive estimator approach proposed in the next sub-section, has been performed.

– interference suppression (IS): this step aims at removing the interference stemming from the as-yet undecoded components. The purpose of this step is hence to filter the $\tilde{u}$th order MMSE-SD residual $\mathbf{Y}_{\tilde{u},i}$. By denoting σ_s^2 the signal power allocated on each of the sub-carriers, $\mathbf{W}_{\tilde{u},i}$ the suppression weight matrix for the selected $\tilde{u}$th user at the ith iteration satisfies [11]:

$$\mathbf{W}_{\tilde{u},i} = \left(\frac{\sigma_b^2}{\sigma_s^2}\mathbf{I} + \mathbf{G}_{\tilde{u},i}^H\mathbf{G}_{\tilde{u},i}\right)^{-1}\mathbf{G}_{\tilde{u},i}^H \tag{17}$$

Then, (17) is used to decode the selected user and to obtain the estimated signal sent by uth user. [5]

$$\hat{\mathbf{S}}_{\tilde{u},i}(k) = \underset{\Omega_m \in}{\text{argmin}} \left\|\mathbf{T}_{\tilde{u},i}(k) - \Omega_m\right\|^2 \tag{18}$$

$$\text{with: } \mathbf{T}_{\tilde{u},i} = \mathbf{Q}_{\tilde{u}}\mathbf{W}_{\tilde{u},i}\mathbf{Y}_{\tilde{u},i}$$

where $\boldsymbol{\Omega} = \{\Omega_1, \Omega_2, \ldots \Omega_m, \ldots \Omega_M\}$ is the modulation constellation. At that stage, (18) makes it possible to obtain the estimated signal of the $\tilde{u}$th user.

$$\hat{\mathbf{A}}_{\tilde{u},i} = \mathbf{H}_{\tilde{u}}\mathbf{Q}_{\tilde{u}}\hat{\mathbf{S}}_{\tilde{u},i} = \left[\hat{A}_{\tilde{u},i}(0), \hat{A}_{\tilde{u},i}(1), \ldots, \hat{A}_{\tilde{u},i}(N-1)\right] \tag{19}$$

In the next section, those estimated signals, the "MMSE-SD preambles" are used to estimate the CFO of each user.

[4] The matrix $\mathbf{H}_{\tilde{u}}$ is assumed to have been estimated using the preamble.

[5] For example in BPSK modulation $\hat{\mathbf{S}}_{\tilde{u},i} = \text{sign}\left(\mathbf{Q}_{\tilde{u}}\mathbf{W}_{\tilde{u},i}\mathbf{Y}_{\tilde{u},i}\right)$.

3.2 Optimal Filter Based Estimator

The CFO is estimated by a recursive method. Let us introduce the state-space model to estimate the CFO, that is the representation of what happens during one OFDMA symbol. It is defined by the following state-space model:

State equation:

$$\epsilon_{\tilde{u},i}(n) = \epsilon_{\tilde{u},i}(n-1) + w(n) \tag{20}$$

Measurement equation:

$$\begin{aligned} \hat{R}_{\tilde{u},i}(n) &= \hat{A}_{\tilde{u},i}(n) e^{j2\pi n \epsilon_{\tilde{u},i}(n)/N} + B_{\tilde{u}}(n) \\ &= f(\epsilon_{\tilde{u},i}(n)) + B_{\tilde{u}}(n) \end{aligned} \tag{21}$$

where w and $B_{\tilde{u}}$ are white zero-mean gaussian noises with variances assumed to be σ_w^2 and $\sigma_{\tilde{u}}^2$ respectively. It should be noted that σ_w^2 is very low and can even be equal to 0. In this latter case, the CFO is assumed to be constant during one OFDMA symbol.

Let us introduce a third state-space equation that is used in the general case for H_∞ filtering to focus on a linear combination of the state-vector components. Here, as the dimension of the state vector is equal to 1, one has:

$$z_{\tilde{u},i}(n) = L\epsilon_{\tilde{u},i}(n) \tag{22}$$

where L is equal to 1.

As the state-space model is non-linear due to (21), we suggest studying four kinds of algorithms:

- The EKF [21] consists in analytically propagating the Gaussian Random Variable (GRV) through the system dynamics, by means of a first-order linearization (Taylor expansion) of the non-linear Eq. (21) around the last available estimate of the state vector. See Appendix A. However, due to the first-order approximation, the EKF may sometimes lead to large errors when evaluating the mean and the covariance matrix of the GRV that undergoes the non-linear transform.
- When dealing with the SPKF [18], the state distribution is still approximated by a Gaussian distribution, but is now characterized by a set of points lying along the main eigenaxes of the GRV covariance matrix. Then, these so-called sigma points propagate through the non-linear system (21). A weighted combination of the resulting values makes it possible to estimate the mean and the covariance matrix of the transformed random vector, i.e. the random variable that undergoes the non-linear transformation. On the one hand, the UKF is based on the unscented transformation [18]. When the density is odd, the weights are chosen to provide the exact 2nd order Taylor expansion around the mean of the random variable. On the other hand, the CDKF is based on the 2nd order Sterling polynomial interpolation formula. Note that when using the sigma-points approach, we avoid calculating the Jacobian.

  Remark: the UKF was proposed by their authors as an alternative to the EKF to avoid the linearization step. Nevertheless, Lefebvre et al. [22] proved that the sigma point approach corresponds to a weighted statistical linear regression (WSLR). The difference between CDKF and UKF stands in the way the mean and the covariance matrix of the transformed GRV is calculated; the weights are not the same. The CDKF uses only a single scalar scaling parameter as opposed to the three required by the UKF. [6] See Appendix B.

[6] For details about SPKF algorithm, the reader is referred to [18].

– The H_∞ approach was introduced in the field of control engineering in 1981. Its purpose is to minimize the worst possible effects of the disturbances on the estimation error. According to [23], H_∞ estimation is more robust to uncertainties than Kalman filtering-based estimation. No statistical assumptions have to be made on the model noise w and the measurement noise $B_{\tilde{u}}$. They are just assumed to have finite energies. Although H_∞ filter has been widely used in the field of control, less studies have been conducted by the signal processing community for the last years.
Here, as we address a non-linear estimation issue, we suggest using the so-called "extended H_∞ filter". [7] Initial works were conducted by Burl [17]; it consists of a first-order linearization around the last available estimation of the state vector. This filter aims at minimizing the H_∞ norm of the transfer operator that maps the discrete time noise disturbances to the estimation error, as follows :

$$J_{\tilde{u},i}^{\infty} = \sup \frac{\sum_{n=0}^{N-1} \|\hat{z}_{\tilde{u},i}(n) - z_{\tilde{u},i}(n)\|^2}{V^{-1} \sum_{n=0}^{N-1} \|B_{\tilde{u}}(n)\|^2 + W^{-1} \sum_{n=0}^{N-1} \|w(n)\|^2 + \|\hat{\epsilon}_{\tilde{u},i}(0) - \epsilon_{\tilde{u},i}(0)\|^2} \tag{23}$$

where V and W are positive weighting parameters tuned by the designer to achieve performance requirements.
Since the minimization of (23) is often impossible, the following sub-optimal H_∞ problem is usually considered:

$$J_{\tilde{u},i}^{\infty} < \gamma^2 \tag{24}$$

where γ is the prescribed noise attenuation level.
At that stage, the H_∞ estimator is the same as the one defined for the Kalman approaches to update the state estimation, but the state-error variance is updated in a different way. See Appendix A.

To improve the estimation, we use a MAI cancellation strategy as in [5]. The results from the $(n-1)$th recursion are used to estimate and eliminate different users' signals in the nth recursion.

$$\text{MAI estimation: } \hat{R}_{\tilde{u},i}^{(est)}(n) = \hat{A}_{\tilde{u},i}(n) e^{j2\pi n \hat{\epsilon}_{\tilde{u},i}(n-1)/N} \tag{25}$$

$$\text{MAI correction: } \hat{R}_{\tilde{u},i}(n) = R(n) - \sum_{j=1, j\neq\tilde{u}}^{U} \hat{R}_{\tilde{u},i}^{(est)}(n) \tag{26}$$

After some recursions, the algorithm makes its possible to estimate the value of the uth user CFO.

4 Computational Complexity

We now look at the complexity of the frequency synchronization scheme presented in the previous section. We begin with the MMSE-SD step. At each iteration and for each user, the MMSE-SD performs the inversion of a matrix of size $N \times N$ in order to calculate the suppression weight matrix $\mathbf{W}_{\tilde{u},i}$. This matrix inversion requires $\mathcal{O}(N^3)$ operations. Thus, the overall complexity of the MMSE-SD step is $\mathcal{O}(I_{max} U N^3)$.

[7] It should be noted that the unscented H_∞ filter has been recently proposed in [20].

Next, we consider the estimation step. As the dimension of the state vector is equal to 1, the optimal filtering step requires the computation of $\mathcal{O}(1)$ operations for each user and for each iteration. Thus, the overall complexity of the estimation step is $\mathcal{O}(I_{max}U)$. In the following, we choose the SPKF to performs the CFO estimation, in order to avoid the linearization step.

Now, we can conclude that the overall complexity of the proposed iterative architecture is bounded by $\mathcal{O}(I_{max}UN^3)$.

5 Simulation Results

We consider an OFDMA IEEE 802.16 WirelessMAN^{TM} interleaved uplink system, which involves 4 users sharing 512 sub-carriers and with a cyclic prefix set to $N_g = 128$. The carrier frequency is at $f_c = 2.5\,\text{GHz}$ and the channel bandwidth is set to $B = 10\text{MHz}$. The duration of an OFDMA symbol is $T_s = N/B$ and $N_s T_s << T_c$, where T_c is the coherence time of the channel and N_s is the number of OFDMA symbols in the OFDMA frame. The users' normalized CFO errors are due to the difference between the frequency carrier and local oscillators, and also to the users movement. A transmission over a Rayleigh quasi-static frequency selective channel composed of 3 multipaths is supposed. QPSK is used to modulate the information bits. $\gamma = 10^3$; $V = 1$ when using the H_∞ filter. One assumes that there is state noise $w(n)$ with very small variance, e.g. $W = 10^{-3}$ and $\sigma_w^2 = 10^{-3}$.

We assume the channel estimation and a CFO pre-estimation have been performed using the preamble. The algorithm aims at estimating the "MMSE-SD preambles" of the 4 users, and then estimating the CFOs for each OFDMA symbol so that the coherent detection can be robust against variations over all the OFDMA frame. We propose to carry out three kinds of tests.

5.1 Test 1: Recursive Estimation Using Perfectly Estimated MMSE-SD Preambles

In this first case, we assume that the "MMSE-SD preambles" have been perfectly estimated at the receiver. We test our CFO estimation algorithms for users with different CFO. The users' CFO estimation errors are considered fixed during one OFDMA symbol. We perform 500 Monte-Carlo runs. Based on preliminary tests, we notice that the EKF, UKF and CDKF provide very similar results, with the difference that the UKF and the CDKF avoid the linearization step. Therefore, in the following we only show the results obtained when using a SPKF. According to Fig. 6, our approach makes it possible to accurately estimate the CFO recursively using a CDKF. It should be noted this is the recursive estimation of the CFO over only one OFDMA symbol.

5.2 Test 2: Non-Pilot Aided Estimation

In this second case, the receiver estimates the "MMSE-SD preambles". The simulation results are focused on the first user of the system. The users' CFO errors vary between the different OFDMA symbols (but they are considered fixed during one OFDMA symbol). They are modeled as independent zero-mean Gaussian random variables with a variance of σ_{cfo}^2. Figure 7 shows the results in terms of CFO estimation over one OFDMA symbol. The proposed algorithm provides an estimation of the CFO in an iterative way by using an UKF. As expected, the first iteration leads to poor performances, but iterating our approach especially up to 5 times leads to good performances. In Fig. 8, we show the performances of our algorithm in terms of BER. The estimation is done by using either the Kalman filter (KF) with

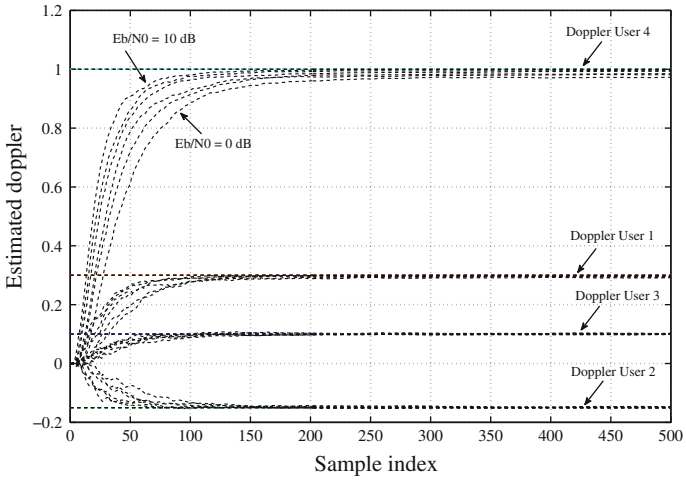

Fig. 6 CDKF approach for CFO estimation with a known preamble

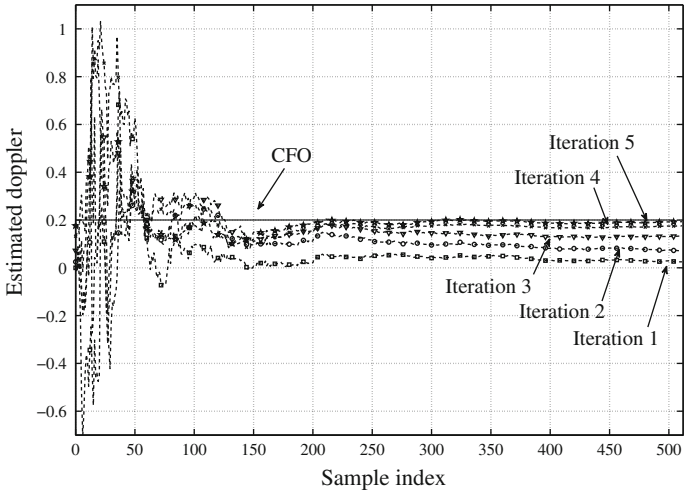

Fig. 7 MMSE-SD combined with UKF approach for CFO estimation

an error of 3 dB over the variance or the H_∞ filter. In addition, we show the results when the direct method is used when considering a perfectly estimated CFOs. We clearly see that the results of the proposed method are better after performing the fourth iteration. A gain of around 1 dB at a BER of 10^{-2} is obtained using the proposed method with the H_∞ filter at the fifth iteration in comparison with the direct method of multiply the complex envelope of the signal before the FFT. In [9] and [10], the algorithms tend to the theoretical value. However in [9], more subchannels than users are required. In addition, a training sequence is required in [10].

In Fig. 9, we show the results in terms of minimum mean square error (MMSE). Based on previous tests, the results in [16] are better than the results in [15] in terms of CFO estimation performances. So we propose a comparative study with the multiuser interference resilient (MUI) approach proposed in [16]. Note that the algorithm proposed in [16] needs

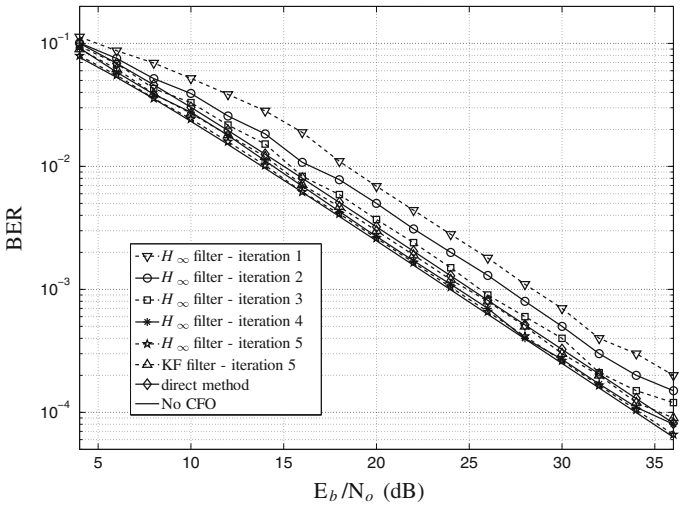

Fig. 8 BER performance, random uniformly distributed CFO, 5 iterations

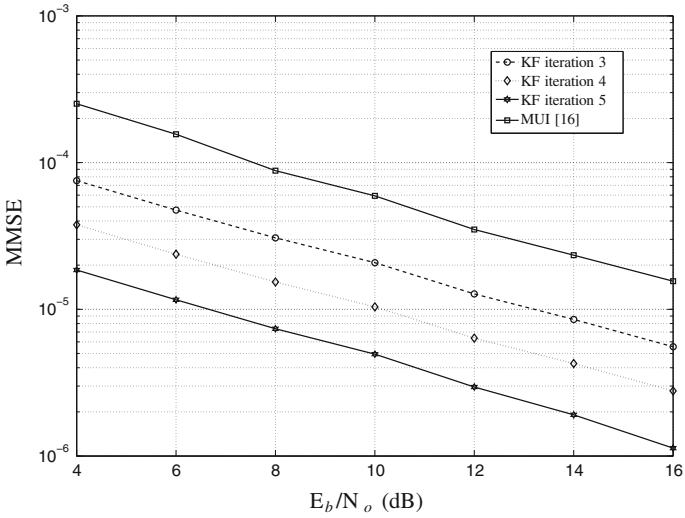

Fig. 9 CFO estimation performances

two OFDMA symbols to do the estimation. A gain of 4 dB at a MMSE of 10^{-4} is obtained between the MUI method and the proposed method at the third iteration using a KF. In addition, in Fig. 10 we compare the KF and the H_∞ filter in terms of convergence speed, for a $E_b/N_o = 10$ dB, for different errors over the noise variance when using the KF and for different values of γ when using the H_∞ filter. Firstly, we consider an error over the variance of 3 and 5 dB. Secondly, we assume no error over the variance. We can see that the convergence speed of the KF is affected by the noise variance error. For the lowest values of γ, the convergence may be slightly faster. If the value of γ increases, the H_∞ filter performances tend to be the same as KF ones. See Appendix A.

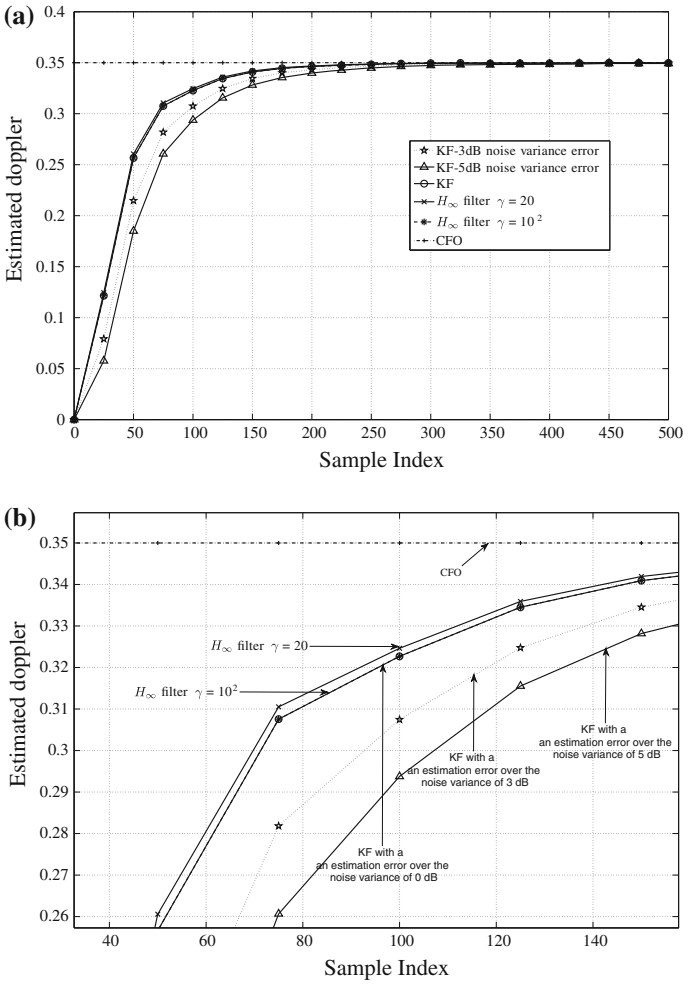

Fig. 10 Comparison of the filters in terms of convergence speed

5.3 Test 3: Influence of the Channel Impulse Response

In this third case, we propose to analyze the influence of the channel impulse responses variations over the receiver performances. The CFO estimation is performed by a KF, knowing the noise characteristics. The simulation results are focused on the first user of the system. We assume that the channel impulse responses have small variations in time over the OFDMA frame. We denote $\hat{\mathbf{h}}_u$ the estimated channel impulse response for each user using the preamble and $\mathbf{h}_{\tilde{u}}$ the real value of the channel response for each user. In a first test, we assume a normalized random error over each symbol $|\hat{\mathbf{h}}_u - \mathbf{h}_{\tilde{u}}| < 10^{-2}$ whereas $|\hat{\mathbf{h}}_u - \mathbf{h}_{\tilde{u}}| < 10^{-1}$ in a second test. The results obtained at the fifth iteration for the different BER with a different error over the channels are shown in Fig. 11. One can notice that the performances of the architecture are not really affected by a small variations on the channel.

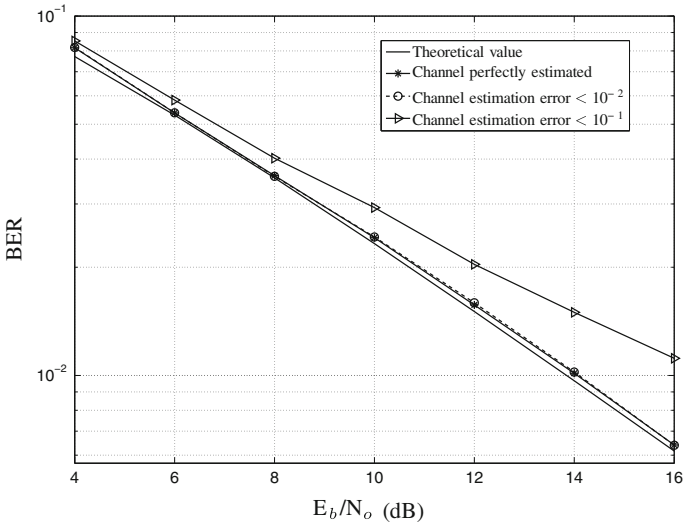

Fig. 11 BER performance, error over the channel estimation

6 Conclusions and Perspectives

The non-pilot aided MAI suppression scheme for an interleaved OFDMA uplink transmission followed by the CFO estimation algorithm based on optimal filtering can jointly estimate and detect respectively each user's CFO and frame, with no need of pilot sub-carriers. This enables a maximum transmission data rate.

In addition, simulation results demonstrate that the proposed scheme can effectively suppress the MAI caused by a relatively large CFO, sufficiently robust to CFO variations. The decoding of interleaved OFDMA is an ordered serial processing that combines interference suppression and interference cancellation techniques. The iterative decoding applies simple hard interference cancellation techniques, resulting in moderate complexity.

The CFO estimation performances of the four different approaches give quite similar results. On the one hand, one advantage of the SPKF is that it does not need the calculations of Jacobians or Hessians. In those cases, the computational complexity is lower. On the other hand, when using the H_∞ filter, no information about the noise statistics is required.

Acknowledgments We would like to thank Pedro Ramos from the University of Zaragoza-Communication Technologies Group, for the fruitful discussions we had with him concerning sigma point Kalman filtering. This work was partially supported by the National Bureau of Science, Technology and Innovation of Panama (SENACYT).

Appendix

A Kalman Filter versus H_∞ Filter

In this appendix, our purpose is to compare the H_∞ filter and the KF when estimating model parameters, by comparing the Ricatti equations of both algorithms. Given the state-space representation in (20)–(22).

On the one hand, the KF satisfies the following Riccati equation:

$$P_{\tilde{u},i}(n+1|n) = P_{\tilde{u},i}(n|n) + \sigma_w^2 \tag{27}$$

$$P_{\tilde{u},i}(n|n) = P_{\tilde{u},i}(n|n-1) - K_{\tilde{u},i}(n)\Psi_{\tilde{u},i}(n)P_{\tilde{u},i}(n|n-1) \tag{28}$$

where $P_{\tilde{u},i}(n|n)$ and $P_{\tilde{u},i}(n|n-1)$ are the *a posteriori* and the *a priori* error variances at time n for the $\tilde{u}$th user at the ith iteration, $\Psi_{\tilde{u},i}(n) = \frac{\partial f(\epsilon_{\tilde{u},i})}{\partial \epsilon_{\tilde{u},i}}|_{\epsilon_{\tilde{u},i}=\hat{\epsilon}_{\tilde{u},i}(n-1)} = \frac{j2\pi n}{N} e^{\frac{j2\pi \hat{\epsilon}_{\tilde{u},i}(n-1)}{N}}$ and $K_{\tilde{u},i}(n) = P_{\tilde{u},i}(n|n-1)\Psi^*_{\tilde{u},i}(n)\Lambda_{\tilde{u},i}(n)^{-1}$ is the Kalman gain of the filter, with $\Lambda_{\tilde{u},i}(n) = \Psi_{\tilde{u},i}(n)P_{\tilde{u},i}(n|n-1)\Psi^*_{\tilde{u},i}(n) + \sigma^2_{\tilde{u}}$. The estimation update is given as follows:

$$\hat{\epsilon}_{\tilde{u},i}(n|n) = \hat{\epsilon}_{\tilde{u},i}(n|n-1) + Re(\chi_{\tilde{u},i}(n)) \tag{29}$$

$$\chi_{\tilde{u},i}(n) = K_{\tilde{u},i}(n)\{\hat{R}_{\tilde{u},i}(n) - f\{\hat{\epsilon}_{\tilde{u},i}(n|n-1)\}\} \tag{30}$$

On the other hand, given weight scalars V and W and provided that:

$$P^{\infty}_{\tilde{u},i}(n+1|n)^{-1} + \Psi^*_{\tilde{u},i}(n)\Psi_{\tilde{u},i}(n) - \gamma^{-2} > 0 \tag{31}$$

the H_∞ filter satisfies:

$$\begin{aligned} P^{\infty}_{\tilde{u},i}(n+1|n) &= P^{\infty}_{\tilde{u},i}(n|n) + W \\ &= P^{\infty}_{\tilde{u},i}(n|n-1)\{1 - \left[\Psi^*_{\tilde{u},i}(n)\ 1\right] \\ &\qquad \times M^{-1}_{\tilde{u},i}\begin{bmatrix}\Psi_{\tilde{u},i}(n)\\ 1\end{bmatrix} P^{\infty}_{\tilde{u},i}(n|n-1)\} + W \end{aligned} \tag{32}$$

where

$$\begin{aligned} M_{\tilde{u},i} &= \begin{bmatrix} V0 \\ 0 - \gamma^2 \end{bmatrix} + \begin{bmatrix}\Psi_{\tilde{u},i}(n)\\ 1\end{bmatrix} P^{\infty}_{\tilde{u},i}(n|n-1)\left[\Psi^*_{\tilde{u},i}(n)1\right] \\ &= \begin{bmatrix} \Psi_{\tilde{u},i}(n)P^{\infty}_{\tilde{u},i}(n|n-1)\Psi^*_{\tilde{u},i}(n) + V & \Psi_{\tilde{u},i}(n)P^{\infty}_{\tilde{u},i}(n|n-1) \\ P^{\infty}_{\tilde{u},i}(n|n-1)\Psi^*_{\tilde{u},i}(n) & P^{\infty}_{\tilde{u},i}(n|n-1) - \gamma^2 \end{bmatrix} \\ K^{\infty}_{\tilde{u},i}(n) &= P^{\infty}_{\tilde{u},i}(n|n-1)\Psi^*_{\tilde{u},i}(n)\{\Lambda^{\infty}_{\tilde{u},i}(n)\}^{-1} \end{aligned} \tag{33}$$

and

$$\Lambda^{\infty}_{\tilde{u},i}(n) = \Psi_{\tilde{u},i}(n)P^{\infty}_{\tilde{u},i}(n|n-1)\Psi^*_{\tilde{u},i}(n) + V \tag{34}$$

Let us first assume that $P^{\infty}_{\tilde{u},i}(n|n-1) = P_{\tilde{u},i}(n|n-1)$. In addition, as it is often done when dealing with H_∞ filter in signal processing, let us set V and W to $\sigma^2_{\tilde{u}}$ and σ^2_w respectively. This implies that $K^{\infty}_{\tilde{u},i}(n) = K_{\tilde{u},i}(n)$ and $\Lambda^{\infty}_{\tilde{u},i}(n) = \Lambda_{\tilde{u},i}(n)$. Then, let us compare $P^{\infty}_{\tilde{u},i}(n+1|n)$ and $P_{\tilde{u},i}(n+1|n)$. For this purpose, $M_{\tilde{u},i}$ must be inverted in (32). Among the approaches that could be considered such as the matrix inversion lemma, we suggest using the one based on the Schur complement [24] for the sake of simplicity. Indeed by defining the Schur complement $\Upsilon_{\tilde{u},i}(n)$ of $\Lambda^{\infty}_{\tilde{u},i}(n)$ in $M_{\tilde{u},i}$ as follows:

$$\begin{aligned}\Upsilon_{\tilde{u},i}(n) &= \{P^{\infty}_{\tilde{u},i}(n|n-1) - \gamma^2\} \\ &\quad - P^{\infty}_{\tilde{u},i}(n|n-1)\Psi^{*}_{\tilde{u},i}(n)\{\Lambda^{\infty}_{\tilde{u},i}(n)\}^{-1}\Psi_{\tilde{u},i}(n)P^{\infty}_{\tilde{u},i}(n|n-1) \\ &= P_{\tilde{u},i}(n|n-1) \\ &\quad - \{P_{\tilde{u},i}(n|n-1)\Psi^{*}_{\tilde{u},i}(n)\{\Lambda_{\tilde{u},i}(n)\}^{-1}\}\Psi_{\tilde{u},i}(n)P_{\tilde{u},i}(n|n-1) - \gamma^2 \\ &= P_{\tilde{u},i}(n|n-1) - K_{\tilde{u},i}(n)\Psi_{\tilde{u},i}(n)P_{\tilde{u},i}(n|n-1) - \gamma^2 \\ &= P_{\tilde{u},i}(n|n) - \gamma^2 \end{aligned} \tag{35}$$

Then, $M^{-1}_{\tilde{u},i}$ can be expressed as the product of three matrices, the coefficients of which are defined from the coefficients of $M_{\tilde{u},i}$ and the Schur complement $\Upsilon_{\tilde{u},i}(n)$ as follows:

$$\begin{aligned} M^{-1}_{\tilde{u},i} &= \begin{bmatrix} 1 & -K^{*}_{\tilde{u},i}(n) \\ 0 & 1 \end{bmatrix} \begin{bmatrix} \Lambda_{\tilde{u},i}(n)^{-1} & 0 \\ 0 & \Upsilon_{\tilde{u},i}(n)^{-1} \end{bmatrix} \begin{bmatrix} 1 & 0 \\ -K_{\tilde{u},i}(n) & 1 \end{bmatrix} \\ &= \Sigma_{\tilde{u},i}(n)\Gamma_{\tilde{u},i}(n)\Xi_{\tilde{u},i}(n) \end{aligned} \tag{36}$$

We can rewrite the Riccati recursion (32) as:

$$\begin{aligned} P^{\infty}_{\tilde{u},i}(n+1|n) &= P_{\tilde{u},i}(n|n-1) + \sigma^2_w \\ -P_{\tilde{u},i}(n|n-1) &\begin{bmatrix} \Psi^{*}_{\tilde{u},i}(n) & 1 \end{bmatrix} \Sigma_{\tilde{u},i}(n)\Gamma_{\tilde{u},i}(n)\Xi_{\tilde{u},i}(n) \begin{bmatrix} \Psi_{\tilde{u},i}(n) \\ 1 \end{bmatrix} P_{\tilde{u},i}(n|n-1) \\ &= P_{\tilde{u},i}(n|n) - P_{\tilde{u},i}(n|n)\{P_{\tilde{u},i}(n|n) - \gamma^2\}^{-1}P_{\tilde{u},i}(n|n) + \sigma^2_w \end{aligned} \tag{37}$$

Hence, since $P_{\tilde{u},i}(n|n)$ is scalar, the solution of the Riccati equation when using the H_∞ filter satisfies:

$$\begin{aligned} P^{\infty}_{\tilde{u},i}(n+1|n) &= P^{\infty}_{\tilde{u},i}(n|n) + \sigma^2_w = P_{\tilde{u},i}(n|n) - \frac{P_{\tilde{u},i}(n|n)^2}{P_{\tilde{u},i}(n|n) - \gamma^2} + \sigma^2_w \\ &= P_{\tilde{u},i}(n|n) + Q^{\gamma}_{\tilde{u},i}(n) + \sigma^2_w = P_{\tilde{u},i}(n|n) + \{\sigma^{\gamma w}_{\tilde{u},i}\}^2 \\ &= P_{\tilde{u},i}(n+1|n) + Q^{\gamma}_{\tilde{u},i}(n) \end{aligned} \tag{38}$$

Therefore, H_∞ filtering can be seen as a Kalman filtering with a model-noise variance equal to $\{\sigma^{\gamma w}_{\tilde{u},i}\}^2 = Q^{\gamma}_{\tilde{u},i}(n) + \sigma^2_w$. If $Q^{\gamma}_{\tilde{u},i}(n) > 0$, $\{\sigma^{\gamma w}_{\tilde{u},i}\}^2 > \sigma^2_w$. For parameter tracking, the larger the state-noise variance is, the easier it is to follow the parameter variations, especially when the parameters are subject to brutal variations. Nevertheless, the larger the noise-model variance is, the larger the variance of the estimated parameters over time is. It should be noted that when γ tends to $+\infty$, $Q^{\gamma}_{\tilde{u},i}$ tends to zero and $P^{\infty}_{\tilde{u},i}(n+1|n)$ tends to $P_{\tilde{u},i}(n+1|n)$.

When we assume that there is no noise model (which means that $\sigma^2_w = 0$) and by using (31) and (38), it can be seen that the H_∞ filter exists only if:

$$\gamma^2(1 + \Psi^{*}_{\tilde{u},i}(n)\Psi_{\tilde{u},i}(n)P_{\tilde{u},i}(n|n)) - 2P_{\tilde{u},i}(n|n) > 0 \tag{39}$$

One has $\Psi^{*}_{\tilde{u},i}(n)\Psi_{\tilde{u},i}(n) = \dfrac{4\pi^2 n^2}{N^2}$ and:

$$\gamma^2 > \frac{2P_{\tilde{u},i}(n|n)}{1 + \dfrac{4\pi^2 n^2}{N^2}P_{\tilde{u},i}(n|n)} \tag{40}$$

Given the range of values that the CFOs may have, *e.g.* $\epsilon_{\tilde{u},i}(n) \in [-1, 1]$, the error variance $P_{\tilde{u},i}(n|n)$ is rather smaller than $N^2/4\pi^2 n^2$ for $n < N - 1$. Therefore,

$\gamma^2 > P_{\tilde{u},i}(n|n)$, $Q^{\gamma}_{\tilde{u},i}(n) > 0$ and $P^{\infty}_{\tilde{u},i}(n+1|n) > P_{\tilde{u},i}(n+1|n)$. In addition since $P_{\tilde{u},i}(n+1|n+1) < P_{\tilde{u},i}(n|n)$, $Q^{\gamma}_{\tilde{u},i}(n+1) < Q^{\gamma}_{\tilde{u},i}(n)$. Therefore, the solution to the Ricatti equation for the H_∞ filter can be seen as an upper bound of the Kalman *a priori* error variance. For parameter estimation, whereas Kalman filtering with no model noise corresponds to the RLS, the equations describing H_∞ filtering corresponds to a Kalman filter with a model noise, the variance of which decreases in time.

B Sigma-Point Kalman Filter

Given the state-space representation in (20) and (21), and when a SPKF is considered, the gain and the error variance are related as follows:

$$P_{\tilde{u},i}(n+1|n) = P_{\tilde{u},i}(n|n) + \sigma_w^2 \tag{41}$$

$$P_{\tilde{u},i}(n|n) = P_{\tilde{u},i}(n|n-1) - K_{\tilde{u},i}(n) P^{\tilde{r}}_{\tilde{u},i}(n) K^*_{\tilde{u},i}(n) \tag{42}$$

where

$$K_{\tilde{u},i}(n) = \{P^{\epsilon\tilde{r}}_{\tilde{u},i}(n)\}\{P^{\tilde{r}}_{\tilde{u},i}(n)\}^{-1}$$

is the gain of the filter, $P^{\epsilon\tilde{r}}_{\tilde{u},i}(n)$ is the covariance between the state prediction error and the innovation $\tilde{r}_{\tilde{u},i} = r_{\tilde{u},i}(n) - \hat{r}_{\tilde{u},i}(n)$, where $r_{\tilde{u},i}(n) = \hat{R}_{\tilde{u},i}(n)$, and $P^{\tilde{r}}_{\tilde{u},i}(n)$ is the innovation variance.

Let us introduce $\rho = 1$, that is the length of the state vector. The first step of the algorithm is to calculate the sigma points:

$$\begin{aligned} X^{\epsilon}_{\tilde{u},i}(n|n-1) &= \left[X^{\epsilon}_{0,\tilde{u},i}(n|n-1)\ X^{\epsilon}_{1,\tilde{u},i}(n|n-1)\ X^{\epsilon}_{2,\tilde{u},i}(n|n-1) \right] \\ &= \left[\hat{\epsilon}_{\tilde{u},i}(n-1)\ \hat{\epsilon}_{\tilde{u},i}(n-1) + \xi\sqrt{P_{\tilde{u},i}(n-1)}\ \hat{\epsilon}_{\tilde{u},i}(n-1) - \xi\sqrt{P_{\tilde{u},i}(n-1)} \right] \end{aligned} \tag{43}$$

- where $\xi = \sqrt{1+\kappa}$, $\kappa = \alpha^2 - 1$ and $10^{-3} < \alpha \leq 1$ when using the UKF
- where $\xi = \sqrt{3}$ when using the CDKF.

Since the state noise is zero, the estimation is updated as follows:

$$\hat{\epsilon}_{\tilde{u},i}(n|n-1) = \Sigma^2_{m=0} w^a_m X^{\epsilon}_{m,\tilde{u},i}(n|n-1) \tag{44}$$

- where $w^a_0 = \kappa/(1-\kappa)$ and $w^a_m = 1/[2(1+\kappa)]$ when using the UKF
- where $w^a_0 = 2/3$ and $w^a_m = 1/6$ when using the CDKF.

The sigma points are propagated through the non-linear function (21):

$$Y^{\epsilon}_{\tilde{u},i}(n|n-1) = f\{X^{\epsilon}_{\tilde{u},i}(n|n-1)\} \tag{45}$$

The measurement equation is updated in time:

$$\hat{r}_{\tilde{u},i}(n) = \Sigma^2_{m=0} w^a_m Y^{\epsilon}_{m,\tilde{u},i}(n|n-1) \tag{46}$$

On the one hand, using the UKF, the covariances are calculated as follows:

$$\begin{aligned} P_{\tilde{u},i}(n|n-1) &= \Sigma^2_{m=0} w^c_m ||X^{\epsilon}_{m,\tilde{u},i}(n|n-1) - \hat{\epsilon}_{\tilde{u},i}(n|n-1)||^2 \\ P^{\tilde{r}}_{\tilde{u},i}(n) &= \Sigma^2_{m=0} w^c_m ||Y^{\epsilon}_{m,\tilde{u},i}(n|n-1) - \hat{r}_{\tilde{u},i}(n)||^2 + \sigma^2_{\tilde{u}} \\ P^{\epsilon\tilde{r}}_{\tilde{u},i}(n) &= \\ &\quad \Sigma^2_{m=0} w^c_m \{X^{\epsilon}_{m,\tilde{u},i}(n|n-1) - \hat{\epsilon}_{\tilde{u},i}(n|n-1)\}\{Y^{\epsilon}_{m,\tilde{u},i}(n|n-1) - \hat{r}_{\tilde{u},i}(n)\}^* \end{aligned}$$

where $w_0^c = w_0^a + 3 - \alpha^2$ and $w_m^c = 1/[2(1+\kappa)]$.

On the other hand, using the CDKF, the covariances are calculated as follows:

$$\begin{aligned} P_{\tilde{u},i}(n|n-1) &= w_1^{c1}||X_{1,\tilde{u},i}^{\epsilon}(n|n-1) - X_{2,\tilde{u},i}^{\epsilon}(n|n-1)||^2 \\ &\quad + w_1^{c2}||X_{1,\tilde{u},i}^{\epsilon}(n|n-1) + X_{2,\tilde{u},i}^{\epsilon}(n|n-1) - 2X_{0,\tilde{u},i}^{\epsilon}(n|n-1)||^2 \\ P_{\tilde{u},i}^{\tilde{r}}(n) &= w_1^{c1}||Y_{1,\tilde{u},i}^{\epsilon}(n|n-1) - Y_{2,\tilde{u},i}^{\epsilon}(n|n-1)||^2 \\ &\quad + w_1^{c2}||Y_{1,\tilde{u},i}^{\epsilon}(n|n-1) + Y_{2,\tilde{u},i}^{\epsilon}(n|n-1) - 2Y_{0,\tilde{u},i}^{\epsilon}(n|n-1)||^2 + \sigma_{\tilde{u}}^2 \\ P_{\tilde{u},i}^{\epsilon\tilde{r}}(n) &= \sqrt{w_1^{c1}P_{\tilde{u},i}(n|n-1)}[Y_{1,\tilde{u},i}^{\epsilon}(n|n-1) - Y_{2,\tilde{u},i}^{\epsilon}(n|n-1)]^* \end{aligned}$$

where $w_m^{c1} = 1/36$ and $w_m^{c2} = 1/18$.

Finally the estimation is updated as follows:

$$\hat{\epsilon}_{\tilde{u},i}(n|n) = \hat{\epsilon}_{\tilde{u},i}(n|n-1) + Re(K_{\tilde{u},i}(n)\{r_{\tilde{u},i}(n) - \hat{r}_{\tilde{u},i}(n)\}) \tag{47}$$

References

1. IEEE Standard (2006) Part 16: Air Interface for Fixed and Mobile Broadband Wireless Access System; Amendment 2: Physical and Medium Access Control Layers for Combined Fixed and Mobile Operation in Licensed Bands, IEEE Std 802.16e-2005. http://ieeexplore.ieee.org/stamp/stamp.jsp?tp=&arnumber=1603394&userType=inst.
2. 3GPP Standard (2009) Technical Specification Group Radio Access Network; Evolved Universal Terrestrial Radio Access (E-UTRA); Physical layer procedures (Release 8), 3GPP TS 36.213 V8.8.0. http://www.etsi.org/deliver/etsi_ts/136300_136399/136304/08.08.00_60/ts_136304v080800p.pdf.
3. Morelli, M., Jay Kuo, C. C., & Pun, M. O. (2007). Synchronization techniques for orthogonal frequency division multiple access (OFDMA): A tutorial review. *Proceedings of the IEEE, 95*, 1394–1427.
4. Morelli, M. (2004). Timing and frequency synchronization for the uplink of an OFDMA system. *IEEE Transaction on Communication, 45*(2), 296–306.
5. Zhao, P., Kuang, L., & Lu, J. (2006). Carrier frequency offset estimation using extended Kalman filter in uplink OFDMA systems. ICC '06, June 2006, vol. 6, pp. 2870–2874.
6. Dai, X. (2007). Carrier frequency offset estimation and correction for OFDMA uplink. *IET Communication, 1*(2), 261–273.
7. Choi, J., Lee, C., Jung, W., & Lee, Y. (2000). Carrier frequency offset compensation for uplink of OFDM-FDMA systems. *IEEE Communication Letters, 4*(12), 414–416.
8. Moose, P. H. (1994). A technique for orthogonal frequency division multiplexing frequency offset correction. *IEEE Transactions on Communications, 42*(10), 2908–2914.
9. Huang, D., & Letaief, K.B. (2005). An interference cancellation scheme for carrier frequency offsets correction in OFDMA systems. *IEEE Transactions on Communications, 53*(7), 1155–1165.
10. Cao, Z. Tureli, U., Yao, Y., & Honan, P. (2004). Frequency synchronization for generalized OFDMA uplink. Globecom '04, Dec. 2004 , pp. 1071–1075.
11. Hou, S. W., & Ko, C. C. (2008). Intercarrier interference suppression for OFDMA uplink in time and frequency selective Rayleigh fading channels. VTC '08, May 2008, pp. 1438–1442.
12. Pun, M. O., Shang-Ho, T., & Jay Kuo, C. C. (2004). An EM-based joint maximum likelihood estimation of carrier frequency offset and channel for uplink OFDMA systems. VTC '04, Sept. 2004, vol. 1, pp. 598–602.
13. Pun, M. O., Shang-Ho, T., & Jay Kuo, C. C. (2004). Joint maximum likelihood estimation of carrier frequency offset and channel for uplink OFDMA systems. Globecom '04, Nov. 2004, vol. 6, pp. 3748–3752.
14. Xiaoyu, F., Minn, H., & Cantrell, C. (2006). Two novel iterative joint frequency-offset and channel estimation methods for OFDMA uplink. GLOBECOM '06, Nov.–Dec. 2006, vol. 3, pp. 1–6.
15. Cao, Z., Tureli, U., & Yao, Y. D. (2004). Deterministic multi-user carrier frequency offset estimation for interleaved OFDMA uplink. *IEEE Transactions on Communications, 52*(9), 1585–1594.
16. Movahedian, M., Yi Ma, M., & Tafazolli, R. (2008). An MUI resilient approach for blind CFO estimation in OFDMA uplink. PIMRC '08, Sept. 2008, pp. 1–5.
17. Burl, J. B. (1998). H_∞ estimation for nonlinear systems. *IEEE Signal Processing Letters, 5*(8), 199–202.

18. Van der Merwe, R. (2004). Sigma-point Kalman filters for probabilistic inference in dynamic state-space models, PhD thesis, OGI School of Science and Engineering, Oregon Health and Science University, Portland, 2004, pp. 35–37, 50–71.
19. Poveda, H., Ferré, G., Grivel, E., & Ramos, P. (2009). A blind iterative carrier frequency offset estimator based on a Kalman approach for an interleaved OFDMA uplink system. EUSIPCO '09, Aug. 2009, pp. 378–382.
20. Li, W., & Jia, Y. (2010). H-infinity filtering for a class of nonlinear discrete-time systems based on unscented transform. *Signal Processing, 90*(12), 3301–3307.
21. Haykin, S. (1996). *Adaptative filter theory* (pp. 328–333). Englewood: Prentice Hall.
22. Lefebvre, T., Bruyninckx, H., & De Schutter, J. (2002). Comment on a new method for the nonlinear transformation of means and covariances in filters and estimators. *IEEE Transactions on Automatic Control, 47*(8), 1406–1408.
23. Hassibi, B., Sayed, A. H., & Kailath, T. (1999). *Indefinite-quadratic estimation and control, a unified approach to H_2 and H_∞ theories*. Philadelphia: Society for Industrial and Applied Mathematics (SIAM).
24. Brezinski, C. (1988). Other manifestations of the Schur complement. *Linear Algebra and Its Applications, 111*, 231–247.

Author Biographies

Héctor Poveda received the diploma of engineer in electronics and telecommunications in 2006 from the Technological University of Panama (Panama) and his MSc degree in digital signal and image processing from the University of Bordeaux (France) in 2008. He is currently with the Signal and Image Research Group at IMS Laboratory, University of Bordeaux. His research interests are in wireless communication theory including the design of estimation approaches estimation for multi-carrier systems.

Guillaume Ferré received the diploma of engineer in electronics and telecommunications engineering (ENSIL) at the University of Limoges (France) in 2003 and received the PhD degree in 2006 from the Limoges University of Technology. From 2006 to 2008 he worked as senior researcher at Xlim and IMS Laboratories. He is currently associate professor at the ENSEIRB-MATMECA engineer school of Bordeaux (France). His main research interests are in wireless communication theory, including synchronization and channel estimation for multi-carrier systems.

Eric Grivel received the diploma of engineer in electronics in 1996 and the PhD degree in signal processing from the University of Bordeaux (France) in 2000. He is currently an Associate Professor with the Telecommunications Department at the ENSEIRB-MATMECA, a graduate national engineering school in Bordeaux. He also belongs to the Signal and Image Research Group at IMS Laboratory, University of Bordeaux. His research interests include the design of estimation and detection approaches for signal processing with applications in mobile communication, speech processing, radar, etc.